



OPEN

Biosynthesized $\text{BiFe}_2\text{O}_4@Ag$ nanoparticles mediated *Scenedesmus obliquus* induce apoptosis in AGS gastric cancer cell line

Hossein Shamsi¹, Reza Yari²✉ & Ali Salehzadeh¹✉

The use of magnetic metal nanoparticles has been considered in cancer treatment studies. In this study, $\text{BiFe}_2\text{O}_4@Ag$ nanoparticles were synthesized biologically by *Scenedesmus obliquus* for the first time and their anticancer mechanism in a gastric cancer cell line was characterized. The physicochemical properties of the nanoparticles were evaluated by Fourier transform infrared spectroscopy (FT-IR), X-ray diffraction (XRD), energy-dispersive X-ray spectroscopy (EDS), scanning electron microscopy (SEM), transmission electron microscopy (TEM), dynamic light scattering (DLS), and zeta potential analyses. Cell viability and nuclear damage were investigated by the MTT and Hoechst staining assays, respectively. Flow cytometry analysis was performed to determine the frequency of the necrotic and apoptotic cells as well as cell cycle analysis of the nanoparticles-treated cells. Physicochemical characterization showed that the synthesized particles were spherical, without impurities, in a size range of 38–83 nm, with DLS size and zeta potential of 295.7 nm and -27.7 mV, respectively. $\text{BiFe}_2\text{O}_4@Ag$ nanoparticles were considerably more toxic for the gastric cancer cells (AGS cell line) than HEK293 normal cells with IC_{50} of 67 and 117 $\mu\text{g/ml}$, respectively. Treatment of AGS cells with the nanoparticles led to a remarkable increase in the percentage of late apoptosis (38.5 folds) and cell necrosis (13.4 folds) and caused cell cycle arrest, mainly at the S phase. Also, nuclear fragmentation and apoptotic bodies were observed in the gastric cancer cells treated with the nanoparticles. This study represents $\text{BiFe}_2\text{O}_4@Ag$ as a novel anticancer candidate against gastric cancer that can induce cell apoptosis through DNA damage and inhibition of cell cycle progression.

Keywords AGS cell line, Apoptosis, $\text{BiFe}_2\text{O}_4@Ag$ nanoparticles, Cell cycle, Flow cytometry

Gastric cancer is known as one of the most common types of cancer in many parts of the world. The increase in the number of incidences and mortality by this disease has raised serious health concerns¹. Current treatment methods include surgery to remove the cancerous tissues and the use of chemotherapy drugs. However, current treatments lack sufficient efficacy in advanced disease cases and metastatic types. This has led researchers to study the field of designing and testing novel and effective drugs against this disease.

Use of metal nanoparticles has been proposed as a new approach in cancer treatment studies. Many metal elements, when synthesized on a nano-scale, may gain new properties such as increased reactivity and improved permeability, which can be used in various fields^{2,3}. However, the use of such compounds in biomedical fields is not always successful. The clinical use of such compounds faces limitations due to their potential toxic effects or low efficacy⁴. In addition, due to their small size, they can be distributed and accumulated in non-target tissues and cause unwanted side effects. Therefore, the design and application of multifunctional nanocomposites can be considered a leading step in the field of using metal nanoparticles in biomedical applications. In this approach, several nanoparticles can be conjugated to provide a more efficient and less toxic composite. The use of magnetic nanoparticles, such as iron oxide nanoparticles, in the fabrication of such composites can provide directed delivery to the target tissues using an external magnetic force, and in this way, in addition to improving the effectiveness of the nanocomposite, it may reduce drug toxicity by reducing the dispersion and

¹Department of Biology, Rasht Branch, Islamic Azad University, Rasht, Iran. ²Department of Biology, Borujerd Branch, Islamic Azad University, Borujerd, Iran. ✉email: reza.yari@iau.ac.ir; salehzadeh@iaurasht.ac.ir

accumulation of particles in non-target tissues⁵. However, the level of toxicity for healthy cells, biodistribution, stability, immune responses and clearance are among the most important challenges that must be considered in the clinical application of metal nanocomposites.

Biological synthesis is another approach to obtaining less toxic metal nanoparticles to be used in biomedical fields. Unlike physicochemical methods, which use toxic substances and harsh conditions for the synthesis of nanoparticles, in the biological method, living organisms or their products are used in the synthesis of nanoparticles^{6,7}. Algae are a group of autotrophic organisms with economic and ecological importance. Algae are used for the synthesis of nanoparticles as they have a high potential to accumulate metal, are easy to handle and cultivate, can grow at low temperatures, and are less toxic to the environment. The use of algae is mainly due to their high capacity to take in metals and reduce metal ions, relatively low production costs, and most importantly their ability to produce nanoparticles at a large scale⁸. The use of algae extracts is among the most common methods of biological synthesis of metal nanoparticles. *Scenedesmus obliquus* is an algal species that has shown great potential to be used in various fields of biotechnology, including the removal of chemical pollutants and biofuel production. In addition, recent studies have shown that the *S. obliquus* extract can be used to synthesize metal nanoparticles⁹.

Bismuth complexes have shown medicinal properties, including antifungal, antibacterial, and anticancer activities¹⁰. Recent studies have shown that bismuth nanoparticles can prevent the proliferation of cancer cells by inducing the production of reactive oxygen species and the generation of oxidative stress^{11,12}. In a previous work, Hernandez-Delgado et al.,¹³ reported that bismuth nanoparticles induced dose-dependent growth inhibition of breast cancer cells and found that breast cancer cells were more vulnerable than healthy breast cells. They found that bismuth nanoparticles reduce plasma membrane integrity and exert genotoxic effects on breast cancer cells. In addition, Ahamed et al.,¹⁴ found that exposure to Bismuth oxide nanoparticles generates oxidative stress in breast cancer cells, leading to increased lipid peroxidation, GSH depletion, and reduced SOD activity. Furthermore, the nanoparticles caused an apoptotic response in treated cells that were associated with impaired regulation of *Bcl-2*, *Bax*, and *caspase-3* genes. Furthermore, silver nanoparticles are known as biocompatible and effective anticancer agents against various cancer cells^{14,15}. The anticancer mechanism of silver nanoparticles mainly depends on the alteration of cellular redox status which can damage cellular structures such as cytoplasmic membrane and nucleic acid, which results in proliferation inhibition¹⁷⁻¹⁹.

Considering the magnetic properties of Fe_2O_4 and the anticancer potential of bismuth and silver nanoparticles, in this work, $\text{BiFe}_2\text{O}_4@Ag$ nanoparticles were synthesized by *S. obliquus* extract for the first time and their anticancer potential in a gastric cancer cell line was investigated.

Materials and methods

Preparation of *S. obliquus* extract

The *S. obliquus* extract was prepared according to the method described by Salehzadeh et al.¹⁹. To prepare the aqueous extract, 1 g of *S. obliquus* (lyophilized) was added to 50 mL of dH_2O and preserved in incubator at 55 °C for 30 min. Next, the extract was centrifuged at 5000 rpm for 10 min (Kaida, China) and the supernatant was passed through a filter paper. The supernatant was preserved at 4 °C for constructing of $\text{BiFe}_2\text{O}_4@Ag$.

Nanoparticle synthesis

BiFe_2O_4 nanoparticles were synthesized according to the method reported by Salehzadeh et al.¹⁹. At first, 0.2 g of $\text{Bi}(\text{NO}_3)_3$ (5mM) and 0.4 g of $\text{Fe}(\text{NO}_3)_3 \cdot 9\text{H}_2\text{O}$ (10mM) were dissolved in 100 ml of distilled water and the reaction mixture was stirred for 60 min in a water bath at 80 °C. Next, NaOH solution (6 M) was gradually added to the suspension. The suspension was centrifuged and BiFe_2O_4 nanoparticles were harvested, washed, and dried at 70 °C.

In the next step, 40 mg of BiFe_2O_4 nanoparticles and 20 mg of silver nitrate were added to distilled water and the resulting mixture was stirred for 50 min at 55 °C. Then, the *S. obliquus* extract was added to the reaction mixture and stirred overnight at room temperature. Finally, the nanoparticles were separated by centrifugation, washed with ethanol and distilled water, and dried at 70 °C.

Physico-chemical characterization of nanoparticles

Fourier transform infrared spectroscopy (FT-IR)^{20,21}, X-ray diffraction (XRD)²², scanning electron microscopy (SEM)^{23,24} and transmission electron microscopy (TEM)²⁶⁻²⁸, Energy-dispersive X-ray spectroscopy (EDS), zeta potential, and Dynamic Light Scattering (DLS) analyses were used to characterize the physical-chemical properties of the nanoparticles. The functional groups of BiFe_2O_4 and $\text{BiFe}_2\text{O}_4@Ag$ nanoparticles were investigated using FT-IR analysis by a Nicolet IR 100 spectrophotometer (400–4000 cm^{-1}). UV visible spectroscopy was done in the range of 200–800 nm (PerkinElmer, LAMBDA 1050). The crystal structure of the $\text{BiFe}_2\text{O}_4@Ag$ nanoparticle was investigated using a Philips X'Pert MPD diffractometer ($\lambda = 1.54056 \text{ \AA}$) (Cu-K α X-ray tube). The morphologic feature and size of the particles were determined by SEM (TESCAN MIRA3, Czech Republic) and TEM (Zeiss-EM10C-100 kV, Germany) microscopes. EDS assay was done to determine the elemental composition of the nanoparticles (TESCAN Mira3). Furthermore, DLS and zeta potential analyses were performed to determine the hydrodynamic particle size and surface charge of the particles using a Malvern Instruments Ltd, 6.32 device.

Cell culture

Cancer (AGS) and normal (HEK293) cell lines were purchased from the Pasteur Institute of Iran, as gastric cancer and normal human fibroblast cells, respectively. Cell lines were cultured in RPMI 1640 medium (supplemented with 10% FBS, 100 IU/mL penicillin, 100 $\mu\text{g}/\text{mL}$ streptomycin, and 2 mM glutamine) under standard conditions (37 °C, in humidified air containing 5% CO_2).

Cell viability assay

Cytotoxicity of the BiFe₂O₄@Ag nanoparticles for gastric cancer and normal cell lines was assessed by MTT assay^{29–31}. In brief, about 10,000 cells were grown in 96-well plates to reach the 50% confluency and were treated with a concentration gradient (0–500 µg/ml) of the nanoparticles for 24 h. Then, the medium was aspirated, 200 µl of the MTT (2-(4,5-dimethylthiazol-2-yl)-2,5-diphenyltetrazolium bromide) solution was added to the wells, and incubated for four hours. In the next step, the contents of the wells were emptied and 200 µl of DMSO was added and re-incubated for 30 min at room temperature. Finally, the optical absorbance of the wells was measured at 570 nm by a Bio-Rad microplate reader. The inhibitory percentage of the nanoparticles for the studied cell lines was measured using the following formula³⁰. The inhibitory effect of Cisplatin, as a standard anticancer drug, for the AGS cell line was also determined.

$$\text{Inhibition(\%)} = \frac{\text{Abs of control} - \text{Abs of Test}}{\text{Abs of control}} \times 100$$

Flow cytometry assay

Flow cytometry assay was used to study the effect of BiFe₂O₄@Ag nanoparticles on the percentage of healthy, apoptotic, and necrotic cells in AGS cell line. AGS cells were propagated and then, 5 × 10⁵ of cells treated with BiFe₂O₄@Ag nanoparticles at their 50% inhibitory concentration (IC₅₀), while control cells were treated with PBS for 24 h. Thereafter, the cells were washed two times with phosphate-buffered saline and resuspended in binding buffer. Then, the propidium iodide and Annexin V (Roche, Germany) dye was added to cells and incubated for 15 min in dark condition²⁸. Finally, the percentage of healthy, apoptotic, and necrotic cells was measured by the ParTec™ flow cytometry instrument (Germany).

Cell cycle analysis

In order to investigate the changes in the cell content, cell cycle analysis was accomplished by flow cytometry method in cells treated with BiFe₂O₄@Ag nanoparticles. According to procedure of Sigma-Aldrich (USA) Cell Cycle Analysis Kit, the AGS cells were cultured with a density of 5 × 10⁵ in a 6-well plate and subjected to 67 µg/mL of BiFe₂O₄@Ag nanoparticles for 24 h in a CO₂ incubator. In following step, the cells were collected and washed with PBS buffer. Afterward, cold ethanol (70%) was used for fixation, and propidium iodide was used to stain of the cells. Further, the cells were treated with RNase A (100 µg/mL). In the final step, a flow cytometer (ParTec™, Germany) was used to measure the DNA content of the cells.

Hoechst staining

Hoechst staining assay was performed to investigate the nuclear damages caused by BiFe₂O₄@Ag nanoparticles in AGS cells. The AGS cells were grown in 6-well plates with a density of 5 × 10⁵ for 24 h and exposed to 67 µg/mL of BiFe₂O₄@Ag nanoparticles. Subsequent to washing with PBS, the cells were fixed by 4% formaldehyde and then, incubated with Hoechst 33258 (5 µg/ml) at 37 °C for 4h in darkness. Untreated cells were regarded as the control. After washing the cell monolayer with PBS, the cells were examined under a fluorescent microscope (Zeiss, Wetzlar, Germany)³⁰.

Statistical analyses

Statistical analyses were performed by the SPSS. 16.0 software. *one-way ANOVA* analysis was used to evaluate significant differences and the p-value < 0.05 was regarded as statistically significant^{31,32}.

Results

Physicochemical characteristics

According to the FT-IR spectrum of BiFe₂O₄, some vibrations associated with the metal oxide (M–O) bonds can be observed at 474 and 526 cm^{−1}, and the peak at 825 cm^{−1} is related to the C–H bond. Furthermore, two peaks at 1323, and 1383 cm^{−1}, could be related to the stretching vibrations of C–H and N–O bonds. The vibrations associated with the O–H bond can be observed at 3449 cm^{−1}. Characterization of the functional groups of BiFe₂O₄@Ag showed several peaks related to the M–O bond at 227 and 530 cm^{−1}, and stretching bonds at 823, 1079, and 1389 cm^{−1} that are associated with C–H, C–O, and C–H bonds, respectively. The stretching vibration of the C=O bond can be identified at 1648 cm^{−1}. In addition, some vibrations at 2925 and 3444 cm^{−1} are observed which are due to the O–H bonds of the adsorbed water molecules. The results were displayed in Fig. 1.

According to the XRD assay, the peaks at 2θ of 27, 33, and 53 degrees are associated with the Ag atoms, which is in agreement with the JCPDS card No. 89-3722³³. The peak at 2θ of 25 degrees is related to the bismuth atoms³⁴, and the peaks associated with Fe₂O₄ can be found at 30, 35, 42, 45, and 62 degrees³⁵ (Fig. 2).

According to the electron microscope imaging, the synthesized nanoparticles were spherical and within a size range of 38–83 nm. Figure 3 displays the SEM and TEM images of the BiFe₂O₄@Ag nanoparticles. In addition, the zeta potential and DLS size of the particles were −27.7 mV and 295.7 nm (Fig. 4). Characterization of the elemental composition of the BiFe₂O₄@Ag nanoparticles showed that the particles were made of O, Fe, Bi, and Ag atoms and had no elemental impurities. The results were presented in Fig. 5.

MTT assay

The viability of gastric cancer cells and normal human cells after treatment with different concentrations of BiFe₂O₄@Ag nanoparticles was investigated. Our results showed that, although the nanoparticles had dose-dependent toxicity for both cell lines, it was considerably more toxic for the cancer cells than normal ones. The

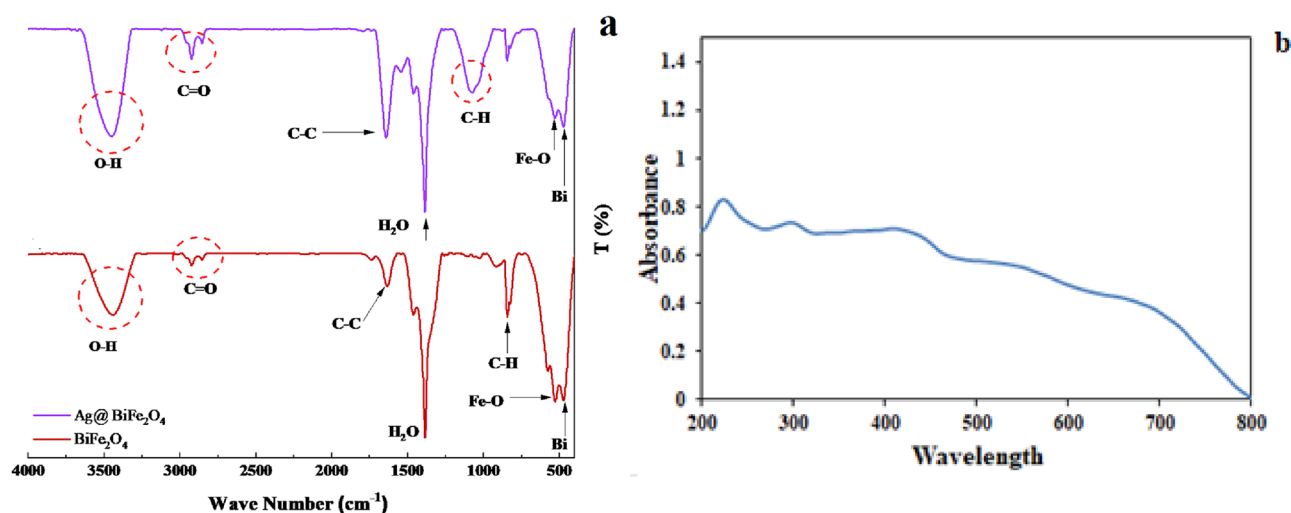


Figure 1. (a) FT-IR analysis of BiFe_2O_4 and $\text{BiFe}_2\text{O}_4@Ag$ nanoparticles. (b,c) UV visible spectroscopy of $\text{BiFe}_2\text{O}_4@Ag$ nanoparticles. Comparing the spectra confirms the formation of the particles.

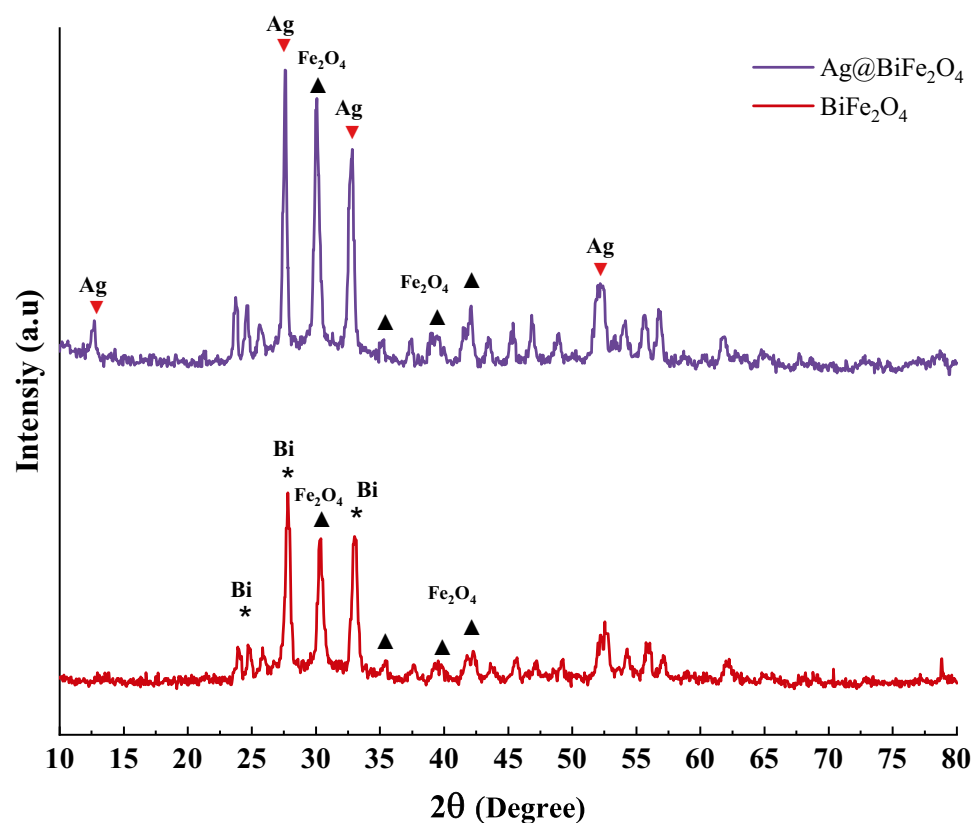


Figure 2. XRD analysis of BiFe_2O_4 and $\text{BiFe}_2\text{O}_4@Ag$ nanoparticles.

50% inhibitory concentration (IC_{50}) of the nanoparticles for the AGS and HEK293 cell lines were 67 and 117 $\mu\text{g}/\text{ml}$, respectively. Furthermore, the IC_{50} of cisplatin for AGS cells was 55 $\mu\text{g}/\text{ml}$. The results were displayed in Fig. 6.

According to the flow cytometry assay, treating gastric cancer cells with $\text{BiFe}_2\text{O}_4@Ag$ nanoparticles led to a remarkable increase in the population of cell necrosis and apoptosis. The highest increase was observed for late apoptosis, which increased from 1.61 to 62.1%, after treatment with the nanoparticles. Furthermore, the percentage of necrotic cells increased from 0.89 to 11.98% (Fig. 7).

Cell cycle analysis

According to the results, upon treatment with the $\text{BiFe}_2\text{O}_4@Ag$ nanoparticles, the frequency of the AGS cells at the G0/M phase was reduced by 25.6%. In contrast, the frequency of the cells arrested at the S phase significantly

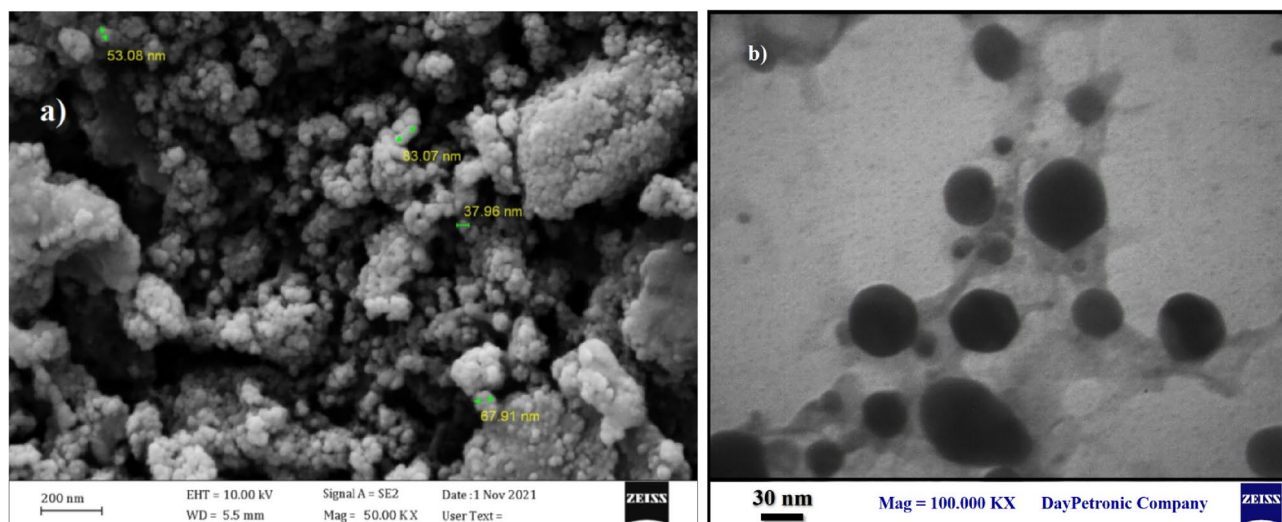


Figure 3. (a) SEM and (b) TEM images of $\text{BiFe}_2\text{O}_4@Ag$ nanoparticles. The particles are spherical and in a size range of 38–83 nm.

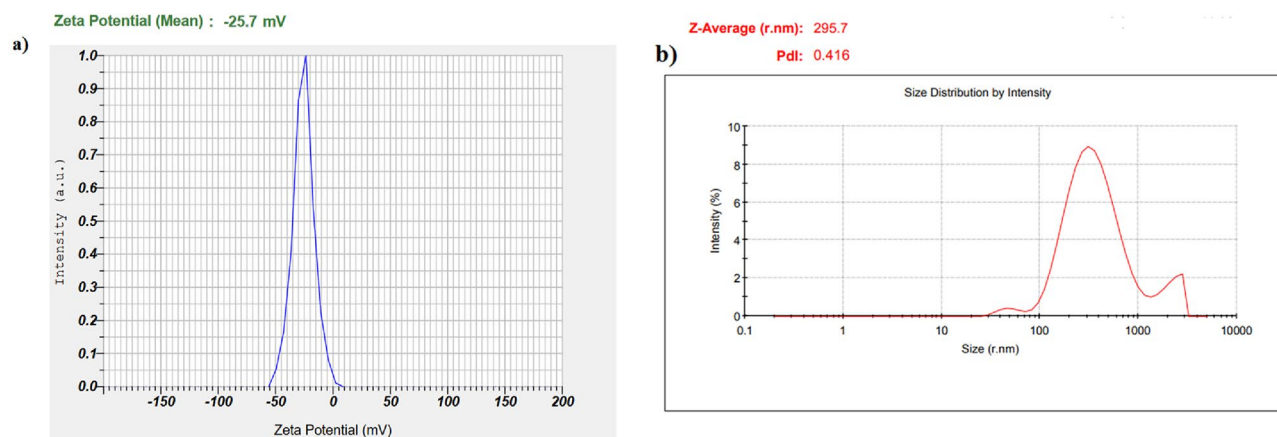


Figure 4. (a) Zeta potential and (b) DLS size of $\text{BiFe}_2\text{O}_4@Ag$ nanoparticles. The surface charge and size of the particles in an aqueous environment were -27.7 mV and 295.7 nm, respectively.

increased from 24.9 to 46.3% (+21.4%). Also, the population of the cells at the G2/M phase was slightly increased after treatment with the nanoparticles (Fig. 8).

Nuclear damage

According to the Hoechst staining assay, after treatment of the AGS cells with $\text{BiFe}_2\text{O}_4@Ag$, some morphological changes favoring apoptosis induction were observed. The main changes include fragmentation of the cell chromatin, formation of apoptotic bodies, as well as condensation of cell chromatin. The results were displayed in Fig. 9.

Discussion

Combination therapies using metallic and magnetic nanoparticles have provided new insight into cancer treatment studies. In this approach, different nanoparticles are combined and manipulated to obtain a nanocomposite with improved efficacy and biocompatibility and less toxicity³⁶. Due to the anticancer potential of silver and bismuth nanoparticles, and the magnetic properties of iron oxide nanoparticles, this work was conducted to synthesize $\text{BiFe}_2\text{O}_4@Ag$ nanoparticles and investigate its effect on a gastric cancer cell line.

Physicochemical characterization of the nanoparticles showed that the particles were synthesized in the nano-scale size range. Nano-size particles have generally large surface areas which can increase their reactivity. Also, due to their small size, they can easily penetrate the host tissues and exert their effects on the target cells. Furthermore, the surface charge of the particles was -27.7 mV which provides enough repulsive force between the particles to avoid particle agglomeration³⁷.

Based on the MTT results, $\text{BiFe}_2\text{O}_4@Ag$ significantly inhibited the growth of the AGS cells. In addition, it had remarkably higher toxicity for the gastric cancer cells than the human normal cell line. The cytotoxic effect of the $\text{BiFe}_2\text{O}_4@Ag$ nanoparticles seems to be mainly associated with its silver and bismuth ions. Many studies

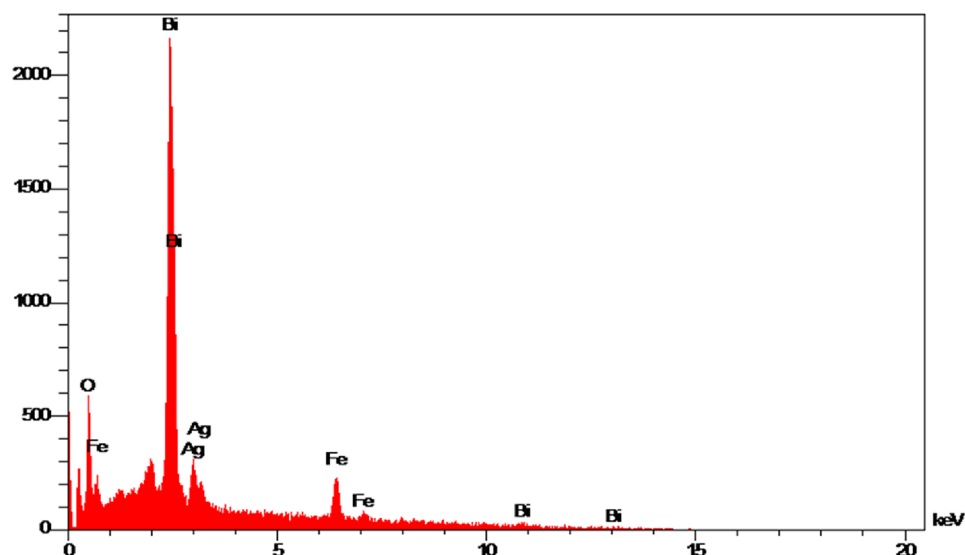


Figure 5. EDS of BiFe₂O₄@Ag nanoparticles. The particles contained Ag, C, O, Fe, and Bi atoms, and elemental impurity was not found.

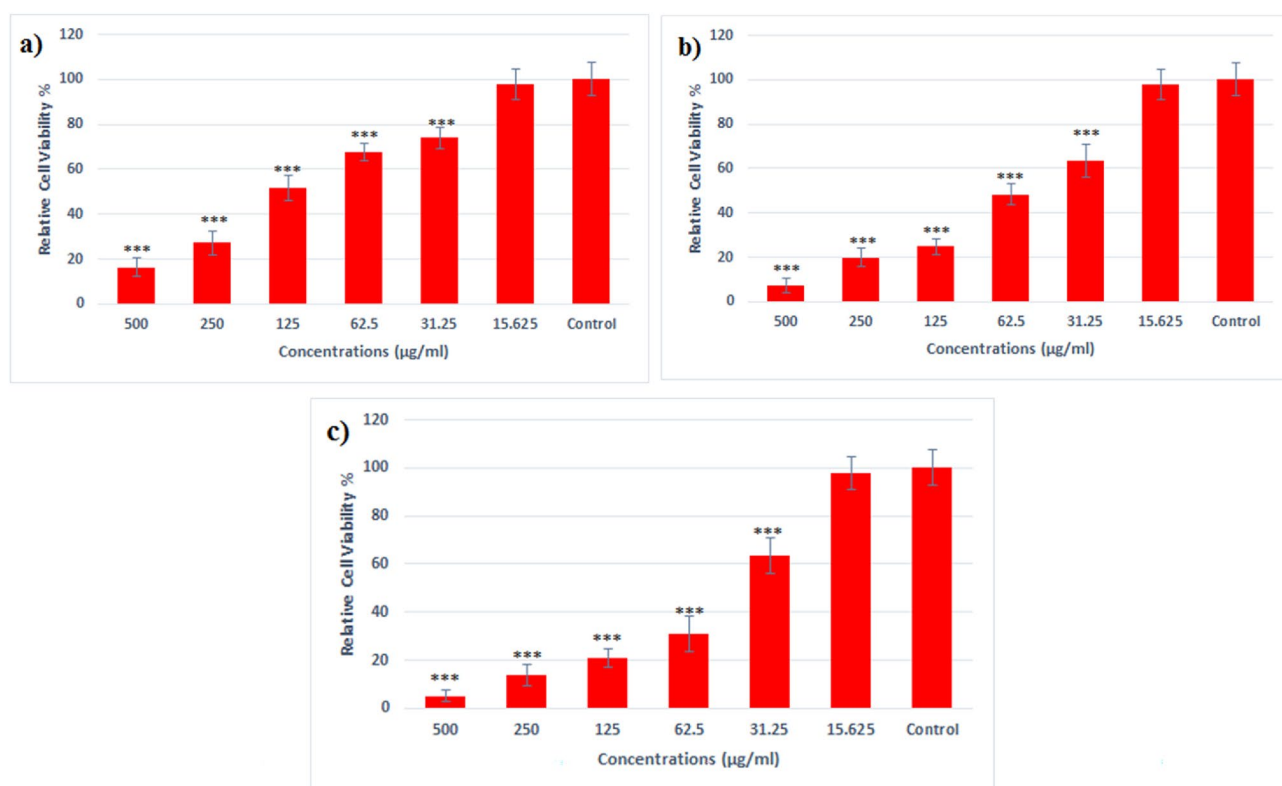


Figure 6. Viability assay for (a) HEK293 cells and (b) AGS cells after treatment with BiFe₂O₄@Ag nanoparticles. (c) Cell viability of AGS cells after treatment with cisplatin. Cancer cells were considerably more susceptible to the nanoparticles than normal cells. The IC₅₀ of BiFe₂O₄@Ag nanoparticles for the normal and cancer cells were 117 and 67 μg/ml, and the IC₅₀ of cisplatin for cancer cells was 55 μg/ml. (***) indicates significant differences at p < 0.001.

have reported the inhibitory effects of silver nanoparticles on various cancer cell lines^{40–42}. Similar to our work, Mousavi et al.⁴⁰ reported dose-dependent toxicity of silver nanoparticles for AGS cell line which considerably inhibited cell proliferation and caused cell apoptosis. Furthermore, it has been reported that bismuth nanoparticles have higher cytotoxicity for cancer cells than healthy cells which is in agreement with our work. It was

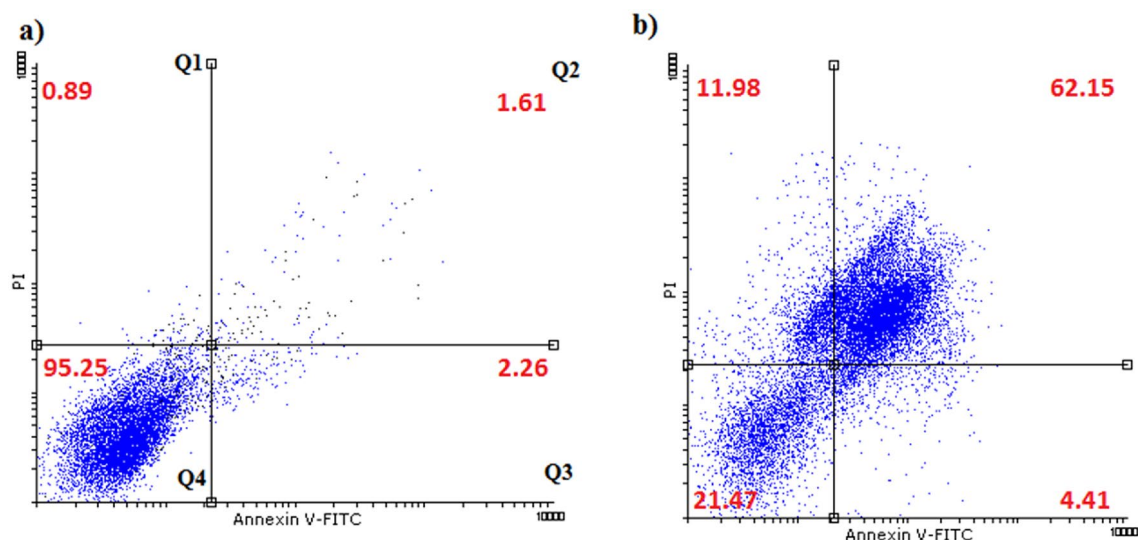


Figure 7. Flow cytometry analysis of AGS cells treated with BiFe₂O₄@Ag nanoparticles. treatment with the nanoparticles significantly increases the population of cell necrosis, primary and late apoptosis. Q1: necrotic cells, Q2: late apoptosis, Q3: primary apoptosis and Q4: live cells.

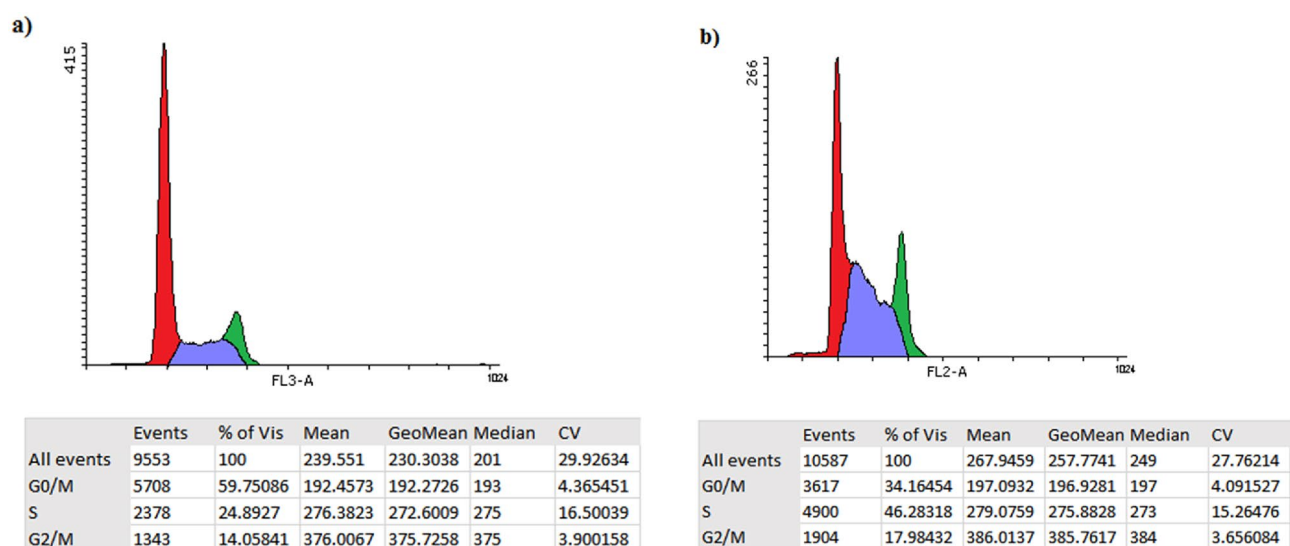


Figure 8. Cell cycle analysis of AGS cells. (a) Control, (b) treated with BiFe₂O₄@Ag nanoparticles. Upon treatment with the BiFe₂O₄@Ag nanoparticles, the frequency of the cells at the G0/M phase was reduced significantly while the population of the cells arrested at the S phase significantly increased.

understood that bismuth nanoparticles can interrupt cytoplasmic membrane integrity and cause DNA damage, leading to cell death¹³.

The inhibitory effect of silver nanoparticles on cancer cells is mainly related to the overproduction of ROS molecules as well as its direct interaction with biological molecules. Previous studies have shown that silver can cause an excessive increase in ROS levels and oxidative stress, which leads to damage to the vital parts of cancer cells, such as the cytoplasmic membrane, DNA molecule, and cellular enzymes, thus inducing apoptosis and cell death^{41,42}. In addition, the increased generation of ROS can modulate signaling pathways such as the mitogen-activated protein kinase (MAPK), phosphoinositide 3- kinase (PI3k)/Akt, and the p53 pathways, leading to cell cycle arrest and apoptosis induction^{43,44}. The generation of oxidative stress in bismuth-treated cells has been reported in the literature^{11,12}. Therefore, damage to cell components by overproduction of ROS molecules seems to be the major cytotoxic mechanism of BiFe₂O₄@Ag nanoparticles in gastric cancer cells.

In addition to oxidative stress, metal nanoparticles can interfere with cell signaling pathways leading to inhibition of cell cycle progression and apoptosis induction. For example, it was found that silver nanoparticles can exert cytotoxic effects on mammalian cells through inhibition of endoplasmic reticulum (ER). The ER functions in protein folding and assembly, lipid biosynthesis and cellular calcium storage. Due to the critical role of ER in cell homeostasis, dysfunction of ER could result in cellular damage and apoptosis. In other words, perturbation

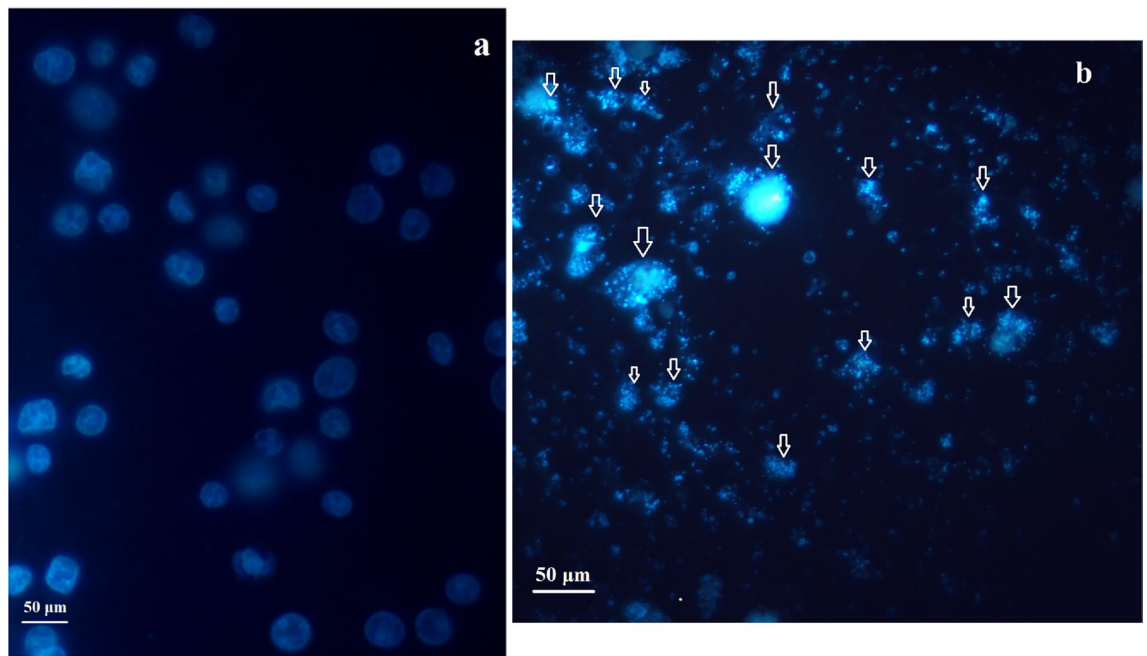


Figure 9. Hoechst staining of AGS cells. (a) Control, (b) BiFe₂O₄@Ag nanoparticles-treated cells. Fragmentation of the cell chromatin, formation of apoptotic bodies, and chromatin condensation were the main observed changes in treated cells.

of the ER function, which is called ER stress, is associated with various cellular damage, leading to ER-induced cell apoptosis and cell death⁴⁵.

The difference in the susceptibility of normal and cancer cells to the nanoparticles can be related to the difference in their metabolic status and proliferation rate. Cancer cells are naturally under higher oxidative stress compared to normal cells due to higher metabolic and hyperproliferation which cause increased ROS generation^{46,47}. For this reason, their tolerance against the excessive production of oxidative radicals is lower than normal cells and their antioxidant systems are less efficient in detoxifying oxidative molecules. Therefore, these cells can be more susceptible to the studied nanoparticles. In a previous study, Sharif et al. reported that gastric cancer cells were considerably more susceptible to oxidative stress generated by GaFe₂O₄@Ag nanoparticles, which is in agreement with our finding¹.

Flow cytometry analysis showed that treatment with BiFe₂O₄@Ag nanoparticles caused a significant increase in cell apoptosis and necrosis. However, the highest increase was observed for the late apoptosis (38.5 folds) suggesting that apoptosis induction is the major anticancer mechanism of the nanoparticles in gastric cancer cells. Previous studies reported that treating various cancer cell lines with silver and bismuth nanoparticles can trigger apoptogenic pathways^{11–47}. Generation of ROS molecules by nanoparticles can cause lipid peroxidation, damage to DNA molecules, and disintegrate mitochondrial and cytoplasmic membranes which in response, triggers apoptotic pathways through the induction of the proapoptotic proteins as well as caspases⁴⁷. Therefore, treating with BiFe₂O₄@Ag nanoparticles seems to initiate apoptosis pathways through the generation of oxidative stress and subsequent damage to the vital components of cancer cells.

Cell cycle analysis showed that treatment with BiFe₂O₄@Ag nanoparticles caused a significant increase in the population of the cells arrested at the S phase. The S phase is the stage before cell division during which the synthesis of DNA and histones occurs. Upon breakage of the DNA molecule, DNA replication will be stopped to activate DNA repair mechanisms. The activation of DNA repair mechanisms leads to a prolonged S phase to provide a longer time to repair DNA molecules⁴⁸. Therefore, the increased population of the cells arrested at the S phase can be related to the cell chromosome damage through the generation of ROS molecules which may result in DNA breakage.

To investigate the possible nuclear damage in the nanoparticles-treated cancer cells, a Hoechst staining assay was performed. The results indicated damage to the cell chromosome which is in agreement with the result from the cell cycle assay. There is a close association between DNA damage and apoptosis⁴⁹. Following extensive damage to the cell's DNA and the inability of the repair systems to repair the damage, apoptotic pathway signals are activated, which initially inhibit cell proliferation and can activate the cascade of caspase proteins, which break down cell proteins and induce cell apoptosis⁴⁶. Therefore, it seems that following damage to the cell's DNA by BiFe₂O₄@Ag nanoparticles, cell proliferation is initially inhibited, mainly at the S phase, and then, apoptotic pathways are triggered in gastric cancer cells. However, conducting additional studies, especially investigating the role of apoptosis signaling molecules, is a limitation of this study, which should be considered in future studies.

Conclusions

In this work, BiFe₂O₄@Ag nanoparticles were synthesized biologically using the *S. obliquus* extract and their anticancer mechanism on a gastric cancer cell line was characterized. Our results showed that the nanoparticles can inhibit the proliferation of the cancer cells, leading to cell cycle arrest at the S phase, and apoptosis induction. This study represents the anticancer potency of BiFe₂O₄@Ag nanoparticles against gastric cancer. However, it is important to acknowledge the limitations of our study including the relevance of *in-vitro* findings to *in-vivo* settings, the optimization of dosage and toxicity profiles, and the assessment of nanoparticle stability and pharmacokinetics.

Data availability

All data generated or analyzed during this study are included in this published article.

Received: 17 November 2023; Accepted: 14 March 2024

Published online: 04 May 2024

References

- Wong, M. C. *et al.* Global incidence and mortality of gastric cancer, 1980–2018. *JAMA Netw. Open* 4(7), e2118457–e2118457. <https://doi.org/10.1001/jamanetworkopen.2021.18457> (2021).
- Jamkhande, P. G., Ghule, N. W., Bamer, A. H. & Kalaskar, M. G. Metal nanoparticles synthesis: An overview on methods of preparation, advantages and disadvantages, and applications. *J. Drug Deliv. Sci. Technol.* 53, 101174. <https://doi.org/10.1016/j.jddst.2019.101174> (2019).
- Umar, H., Kavaz, D. & Rizaner, N. Biosynthesis of zinc oxide nanoparticles using Albizia lebeck stem bark, and evaluation of its antimicrobial, antioxidant, and cytotoxic activities on human breast cancer cell lines. *Int. J. Nanomed.* 1, 87–100. <https://doi.org/10.2147/IJN.S186888> (2019).
- Xu, J. J., Zhang, W. C., Guo, Y. W., Chen, X. Y. & Zhang, Y. N. Metal nanoparticles as a promising technology in targeted cancer treatment. *Drug Deliv.* 29(1), 664–678. <https://doi.org/10.1080/10717544.2022.2039804> (2022).
- Arruebo, M., Fernández-Pacheco, R., Ibarra, M. R. & Santamaría, J. Magnetic nanoparticles for drug delivery. *Nano Today* 2(3), 22–32. [https://doi.org/10.1016/S1748-0132\(07\)70084-1](https://doi.org/10.1016/S1748-0132(07)70084-1) (2007).
- Peralta-Videa, J. R. *et al.* Plant-based green synthesis of metallic nanoparticles: scientific curiosity or a realistic alternative to chemical synthesis?. *Nanotechnol. Environ. Eng.* 1, 1–29. <https://doi.org/10.1007/s41204-016-0004-5> (2016).
- Umar, H. *et al.* Prediction of cell migration potential on human breast cancer cells treated with Albizia lebeck ethanolic extract using extreme machine learning. *Sci. Rep.* 13(1), 22242. <https://doi.org/10.1038/s41598-023-49363-z> (2023).
- Chugh, D., Viswamalya, V. S. & Das, B. Green synthesis of silver nanoparticles with algae and the importance of capping agents in the process. *J. Genet. Eng. Biotechnol.* 19(1), 1–21. <https://doi.org/10.1186/s43141-021-00228-w> (2021).
- Sharif, A. P. *et al.* Cytotoxic effect of a novel GaFe₂O₄@Ag nanocomposite synthesized by *Scenedesmus obliquus* on gastric cancer cell line and evaluation of BAX, Bcl-2 and CASP8 genes expression. *J. Cluster Sci.* 1, 1–11. <https://doi.org/10.1007/s10876-022-02288-5> (2022).
- Gomez, C., Hallot, G., Laurent, S. & Port, M. Medical applications of metallic bismuth nanoparticles. *Pharmaceutics* 13(11), 1793. <https://doi.org/10.3390/pharmaceutics13111793> (2021).
- Ahamed, M., Akhtar, M. J., Khan, M. M., Alrokayan, S. A. & Alhadlaq, H. A. Oxidative stress mediated cytotoxicity and apoptosis response of bismuth oxide (Bi₂O₃) nanoparticles in human breast cancer (MCF-7) cells. *Chemosphere* 216, 823–831. <https://doi.org/10.1016/j.chemosphere.2018.10.214> (2019).
- Alamer, A. *et al.* Bismuth oxide nanoparticles induce oxidative stress and apoptosis in human breast cancer cells. *Environ. Sci. Pollut. Res.* 28(6), 7379–7389. <https://doi.org/10.1007/s11356-020-10913-x> (2021).
- Hernandez-Delgadillo, R. *et al.* In vitro evaluation of the antitumor effect of bismuth lipophilic nanoparticles (BisBAL NPs) on breast cancer cells. *Int. J. Nanomed.* 1, 6089–6097. <https://doi.org/10.2147/IJN.S179095> (2018).
- Sofi, M. A., Sunitha, S., Sofi, M. A., Pasha, S. K. & Choi, D. An overview of antimicrobial and anticancer potential of silver nanoparticles. *J. King Saud Univ. Sci.* 34(2), 101791. <https://doi.org/10.1016/j.jksus.2021.101791> (2022).
- Kavaz, D., Umar, H. & Shehu, S. Synthesis, characterization, antimicrobial and antimetastatic activity of silver nanoparticles synthesized from *Ficus ingens* leaf. *Artif. Cells Nanom. Biotechnol.* 46(sup3), S1193–S1203 (2018).
- Yusuf, A. & Casey, A. Liposomal encapsulation of silver nanoparticles (AgNP) improved nanoparticle uptake and induced redox imbalance to activate caspase-dependent apoptosis. *Apoptosis* 25(1–2), 120–134. <https://doi.org/10.1007/s10495-019-01584-2> (2020).
- Khan, M. S. *et al.* Anticancer potential of biogenic silver nanoparticles: a mechanistic study. *Pharmaceutics* 13(5), 707. <https://doi.org/10.3390/pharmaceutics13050707> (2021).
- Khan, M. S. *et al.* Anticancer potential of biogenic silver nanoparticles: A mechanistic study. *Pharmaceutics* 13(5), 707. <https://doi.org/10.3390/pharmaceutics13050707> (2021).
- Salehzadeh, A., Naeemi, A. S., Khaknezhad, L., Moradi-Shoeili, Z. & Shandiz, S. A. S. Fe₃O₄/Ag nanocomposite biosynthesized using *Spirulina platensis* extract and its enhanced anticancer efficiency. *IET Nanobiotechnol.* <https://doi.org/10.1049/iet-nbt.2018.5364> (2019).
- Khashan, K. S., Jabir, M. S. & Abdulameer, F. A. Preparation and characterization of copper oxide nanoparticles decorated carbon nanoparticles using laser ablation in liquid. *J. Phys. Conf. Ser.* 1003, 12100. <https://doi.org/10.1088/1742-6596/1003/1/012100> (2018).
- Kadhim, W. K. A., Nayef, U. M. & Jabir, M. S. Polyethylene glycol-functionalized magnetic (Fe₃O₄) nanoparticles: A good method for a successful antibacterial therapeutic agent via damage DNA molecule. *Surf. Rev. Lett.* 26(10), 1950079. <https://doi.org/10.1142/S0218625X19500793> (2019).
- Abed, M. A. *et al.* Synthesis of Ag/Au (core/shell) nanoparticles by laser ablation in liquid and study of their toxicity on blood human components. *J. Phys. Conf. Ser.* 1795(1), 12013. <https://doi.org/10.1088/1742-6596/1795/1/012013> (2021).
- Alsaedi, I. I., Taqi, Z. J., Hussien, A. M. A., Sulaiman, G. M. & Jabir, M. S. Graphene nanoparticles induces apoptosis in MCF-7 cells through mitochondrial damage and NF-KB pathway. *Mater. Res. Express* 6(9), 095413. <https://doi.org/10.1088/2053-1591/ab33af> (2019).
- Ali, Z., Jabir, M. & Al-Shammari, A. Gold nanoparticles inhibiting proliferation of Human breast cancer cell line. *Res. J. Biotechnol.* 14, 79–82 (2019).
- Jabir, M. S., Nayef, U. M. & Abdul, K. W. K. Polyethylene glycol-functionalized magnetic (Fe₃O₄) nanoparticles: A novel DNA-mediated antibacterial agent. *Nano Biomed. Eng.* 11(1), 18–27. <https://doi.org/10.5101/nbe.v11i1.p18-27> (2019).

26. Jabir, M. S., Nayef, U. M., Abdulkadhim, W. K. & Sulaiman, G. M. Supermagnetic Fe₃O₄-PEG nanoparticles combined with NIR laser and alternating magnetic field as potent anti-cancer agent against human ovarian cancer cells. *Mater. Res. Express* **6**(11), 115412. <https://doi.org/10.1088/2053-1591/ab50a0> (2019).
27. Ibrahim, A. A. *et al.* Pt (II)-thiocarbohydrazone complex as cytotoxic agent and apoptosis inducer in Caov-3 and HT-29 Cells through the P53 and caspase-8 pathways. *Pharmaceuticals* **14**(6), 509. <https://doi.org/10.3390/ph14060509> (2021).
28. Mahmood, R. I. *et al.* Biosynthesis of copper oxide nanoparticles mediated *Annona muricata* as cytotoxic and apoptosis inducer factor in breast cancer cell lines. *Sci. Rep.* **12**(1), 16165. <https://doi.org/10.1038/s41598-022-20360-y> (2022).
29. Al-Ziaydi, A. G., Al-Shammari, A. M., Hamzah, M. I., Kadhim, H. S. & Jabir, M. S. Hexokinase inhibition using D-Mannoheptulose enhances oncolytic newcastle disease virus-mediated killing of breast cancer cells. *Cancer Cell Int.* **20**, 1–10. <https://doi.org/10.1186/s12935-020-01514-2> (2020).
30. Hosseinkhah, M. *et al.* Cytotoxic potential of nickel oxide nanoparticles functionalized with glutamic acid and conjugated with thiosemicarbazide (NiO@Glu/TSC) against human gastric cancer cells. *J. Cluster Sci.* **1**, 1–9. <https://doi.org/10.1007/s10876-021-02124-2> (2021).
31. Jabir, M. S., Sulaiman, G. M., Taqi, Z. J. & Li, D. Iraqi propolis increases degradation of IL-1 β and NLR4 by autophagy following *Pseudomonas aeruginosa* infection. *Microbes Infect.* **20**(2), 89–100. <https://doi.org/10.1016/j.micinf.2017.10.007> (2018).
32. Jabir, M. S. *et al.* Inhibition of *Staphylococcus aureus* α -hemolysin production using nanocurcumin capped Au@ZnO nanocomposite. *Bioinorg. Chem. Appl.* **1**, 1. <https://doi.org/10.1155/2022/2663812> (2022).
33. Shamel, K. *et al.* Green biosynthesis of silver nanoparticles using *Curcuma longa* tuber powder. *Int. J. Nanomed.* **1**, 5603–5610. <https://doi.org/10.2147/IJN.S36786> (2012).
34. Dadashi, S., Delavari, H. & Poursalehi, R. Optical properties and colloidal stability mechanism of bismuth nanoparticles prepared by Q-switched Nd: Yag laser ablation in liquid. *Proc. Mater. Sci.* **11**, 679–683. <https://doi.org/10.1016/j.mspro.2015.11.027> (2015).
35. ElNahrawy, A. M. *et al.* Impact of Mn-substitution on structural, optical, and magnetic properties evolution of sodium-cobalt ferrite for opto-magnetic applications. *J. Mater. Sci. Mater. Electron.* **31**, 6224–6232. <https://doi.org/10.1007/s10854-020-03176-2> (2020).
36. Patel, M. & Prabhu, A. Smart nanocomposite assemblies for multimodal cancer theranostics. *Int. J. Pharm.* **618**, 121697. <https://doi.org/10.1016/j.ijpharm.2022.121697> (2022).
37. Berg, J. M., Romoser, A., Banerjee, N., Zebda, R. & Sayes, C. M. The relationship between pH and zeta potential of ~30 nm metal oxide nanoparticle suspensions relevant to in vitro toxicological evaluations. *Nanotoxicology* **3**(4), 276–283. <https://doi.org/10.3109/17435390903276941> (2009).
38. Tian, S. *et al.* Anti-cancer activity of biosynthesized silver nanoparticles using *Avicennia marina* against A549 lung cancer cells through ROS/mitochondrial damages. *Saudi J. Biol. Sci.* **27**(11), 3018–3024. <https://doi.org/10.1016/j.sjbs.2020.08.029> (2020).
39. Naik, J. & David, M. ROS mediated apoptosis and cell cycle arrest in human lung adenocarcinoma cell line by silver nanoparticles synthesized using *Swietenia macrophylla* seed extract. *J. Drug Deliv. Sci. Technol.* **80**, 104084. <https://doi.org/10.1016/j.jddst.2022.104084> (2023).
40. Mousavi, B., Tafvizi, F. & Zaker Bostanabad, S. Green synthesis of silver nanoparticles using *Artemisia turcomanica* leaf extract and the study of anti-cancer effect and apoptosis induction on gastric cancer cell line (AGS). *Artif. Cells Nanomed. Biotechnol.* **46**(sup1), 499–510. <https://doi.org/10.1080/21691401.2018.1430697> (2018).
41. Castro-Aceituno, V. *et al.* Anticancer activity of silver nanoparticles from *Panax ginseng* fresh leaves in human cancer cells. *Biomed. Pharmacother.* **84**, 158–165. <https://doi.org/10.1016/j.biopha.2016.09.016> (2016).
42. Hayes, J. D., Dinkova-Kostova, A. T. & Tew, K. D. Oxidative stress in cancer. *Cancer cell* **38**(2), 167–197. <https://doi.org/10.1016/j.ccell.2020.06.001> (2020).
43. Son, Y., Cheong, Y. K., Kim, N. H., Chung, H. T., Kang, D. G., & Pae, H. O. Mitogen-activated protein kinases and reactive oxygen species: how can ROS activate MAPK pathways?. *J. Signal Transduct.* <https://doi.org/10.1155/2011/792639> (2011).
44. Kma, L. & Baruah, T. J. The interplay of ROS and the PI3K/Akt pathway in autophagy regulation. *Biotechnol. Appl. Biochem.* **69**(1), 248–264. <https://doi.org/10.1002/bab.2104> (2022).
45. Zhang, R. *et al.* Endoplasmic reticulum stress signaling is involved in silver nanoparticles-induced apoptosis. *Int. J. Biochem. Cell Biol.* **44**(1), 224–232. <https://doi.org/10.1016/j.biocel.2011.10.019> (2012).
46. Pan, Z. *et al.* Cinobufagin induces cell cycle arrest at the S phase and promotes apoptosis in nasopharyngeal carcinoma cells. *Biomed. Pharmacother.* **122**, 109763. <https://doi.org/10.1016/j.biopha.2019.109763> (2020).
47. Redza-Dutordoir, M. & Averill-Bates, D. A. Activation of apoptosis signalling pathways by reactive oxygen species. *Biochim. Biophys. Acta Mol. Cell Res.* **1863**(12), 2977–2992. <https://doi.org/10.1016/j.bbamcr.2016.09.012> (2016).
48. Barkley, L. R., Ohmori, H. & Vaziri, C. Integrating S-phase checkpoint signaling with trans-lesion synthesis of bulky DNA adducts. *Cell Biochem. Biophys.* **47**, 392–408. <https://doi.org/10.1007/s12013-007-0032-7> (2007).
49. Cao, J. J. *et al.* Anticancer cyclometalated iridium (III) complexes with planar ligands: Mitochondrial DNA damage and metabolism disturbance. *J. Med. Chem.* **62**(7), 3311–3322. <https://doi.org/10.1021/acs.jmedchem.8b01704> (2019).

Author contributions

A.S.: conceptualization. A.S.: methodology. H.S.H., R.Y. and A.S.: formal analysis and investigation. R.Y. and A.S.: editing. H.S.H.: writing original draft preparation. R.Y. and A.S.: editing. H.S.H.: resources. R.Y. and A.S.: supervision. The authors give the publisher the permission to publish this work.

Competing interests

The authors declare no competing interests.

Additional information

Correspondence and requests for materials should be addressed to R.Y. or A.S.

Reprints and permissions information is available at www.nature.com/reprints.

Publisher's note Springer Nature remains neutral with regard to jurisdictional claims in published maps and institutional affiliations.



Open Access This article is licensed under a Creative Commons Attribution 4.0 International License, which permits use, sharing, adaptation, distribution and reproduction in any medium or format, as long as you give appropriate credit to the original author(s) and the source, provide a link to the Creative Commons licence, and indicate if changes were made. The images or other third party material in this article are included in the article's Creative Commons licence, unless indicated otherwise in a credit line to the material. If material is not included in the article's Creative Commons licence and your intended use is not permitted by statutory regulation or exceeds the permitted use, you will need to obtain permission directly from the copyright holder. To view a copy of this licence, visit <http://creativecommons.org/licenses/by/4.0/>.

© The Author(s) 2024